

# Seasonality of temperature, salinity obtained from hydrography observations around South Korea

Eun Ae Lee<sup>1\*</sup> and Sung Yong Kim<sup>1</sup>

<sup>1</sup> Department of Mechanical Engineering, Korea Advanced Institute of Science and Technology, Republic of Korea  
\*eunae.lee@kaist.ac.kr

KAIST

KETEP 한국에너지기술연구원 에너지인력양성사업

## 1. Abstract

We investigate the seasonal variability of temperature, salinity, and geostrophic circulation around South Korea (East/Japan Sea (ES), South coast (SC), and Yellow Sea (YS)) by analyzing conductivity-temperature-depth (CTD) profiles for recent 20 years (1995 to 2014). In the estimates of seasonal amplitudes using harmonic analysis, their accuracy is quantified with how well the seasonal regression reconstructs the known pure seasonal signals with noise. Over the shelf (within 70 km of the coast) in the East Sea, the seasonal amplitudes, means, and root-mean-squares (rms) of subsurface temperature and salinity are about 20-50% smaller than those offshore. Conversely, in the Yellow Sea, the seasonal amplitudes of subsurface temperature onshore waters (within 40 km) become about 40% larger than offshore as a result of enhanced onshore tidal mixing. The vertical diffusivity obtained from annual amplitudes or phases indicates different between coast and offshore.

## 2. Data and Methods

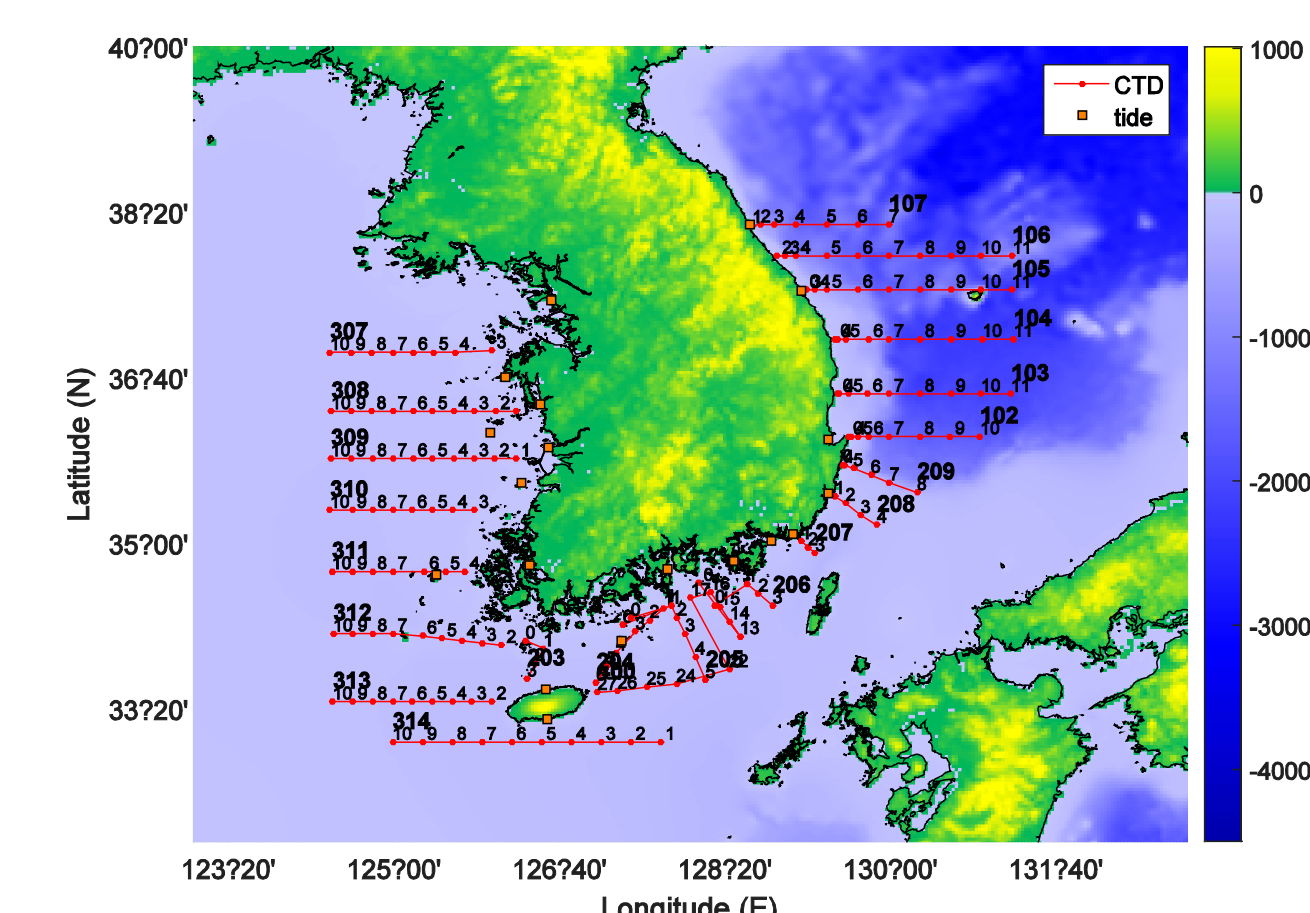


Fig. 1. Historical hydrographic survey lines and stations around Korea

### 2.1. Hydrographic survey data

As a part of periodic hydrographic surveys around Korea, the conductivity-temperature-depth (CTD) data have been sampled six times a year for recent 15 years (2000-2014) by National Fisheries Research and Development Institute (NFRDI). The surveys have been conducted along cross-shore lines off eastern (East Sea), western (Yellow Sea), and southern (Jeju and Korea Strait) areas of the Republic of Korea, within approximately 200 km from the coast (Fig. 1.). The CTD stations are located with a spacing of 0.5° and 1° in the meridional and zonal directions, respectively. The data at a single CTD profile are interpolated at common vertical depths (0, 5, 15, 25, 35, . . . , 480, and 500 m). Additionally, since the salinity data have outliers, are removed through comparing with near station and checking time series.

### 2.2. Regression

A time series ( $d(t)$ ) of temperature (or salinity) at a single depth and location are decomposed into a sum of time-mean ( $\langle d(t) \rangle$ ) seasonal components ( $d_S$ ), and linear trend ( $d_L$ ), and residuals ( $d_R$ )

$$d(t) = \langle d(t) \rangle + d_S(t) + d_L(t) + d_R(t),$$

$$= \langle d(t) \rangle + [G_S G_L] \begin{bmatrix} m_S \\ m_L \end{bmatrix} + d_R(t),$$

where  $G_S$  is the basis functions for seasonal and semi-seasonal frequencies and  $G_L$  is the linear trend basis function. Their corresponding coefficients are  $m_S$  and  $m_L$  respectively. The mean value from CTD observation is biased because of irregular observation time, so a bias is estimated through seasonal and semi-seasonal fit and subtracted. The accuracy of seasonal regression results obtained from unevenly sampled in-situ observations will be discussed in Appendix.

## 3. Results

### 3.1. Time mean and variability

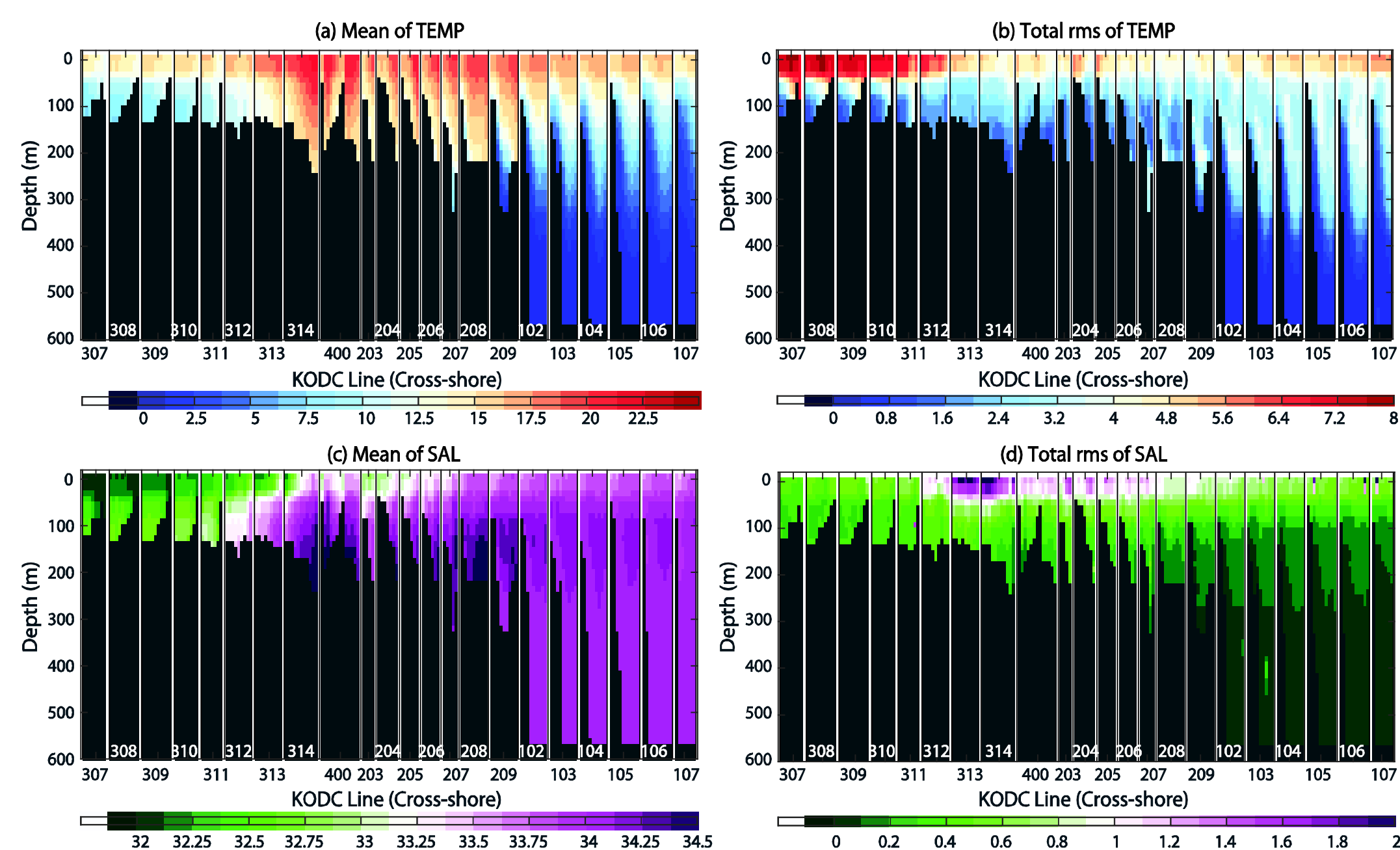


Fig. 2. Mean and rms of temperature (°C) and salinity profiles for recent 20 years (1995 to 2014)

The time mean of temperature profiles shows a downward toward offshore in the upper 300m at the ES are associated with southward undercurrents which is the North Korea cold current (NKCC) and northward surface and offshore current which is Tsushima warm current (TWC). The southward NKCC contains cold, fresh, and oxygen rich water originating from Liman cold current, whereas northward TWC carries warmer, saltier, and oxygen-poor water originating from the Kuroshio current [e.g., Kim and Chung, 1984]. The subsurface isothermal line slopes upward to the north since influence of TWC is getting reduced which causes eastward geostrophic current.

The vertical temperature gradients of time-averaged mean in the SC are weaker than other areas. The horizontal gradients of cross-shore are tilted toward onshore due to TWC and located at low latitude which may generate eastward geostrophic current.

The offshore isothermal lines at the YS is flat along cross-shore since the cold bottom water exist all the year over (which is called the Yellow sea cold bottom water during summer [e.g., Wang et al, 2014]). In addition, the onshore isothermal line is tilted toward onshore which cause weak southward geostrophic current.

The means of salinity at the ES has maximum value between 100 m and 300 m since surface current (salty TWC) between 0 and 100 m is affected by Chang-jiang river and precipitation [e.g., Kang and Jin, 1984]. Additionally, that maximum salinity is shown on 20 km from coast since NKCC move southward along the ES [e.g., Cho and Kim, 1994].

The salinity front exist between the YS and the East China Sea which is related that TWC intrudes to the YS [e.g., Pang and Hyun, 1996]. The low time-averaged salinity about 31 at shore stations (1-2 stations from the coast) tend to appear due to fresh water input from local rivers. For example, line 307, 308, and 309 are related to Asan bay and Guem river.

The salinity front at line 203, 204, and 205 appears because fresh coastal water and salty TWC are encountered [e.g., Yang et al, 1998; Son et al, 2010].

### 3.2. Seasonal amplitudes and phases

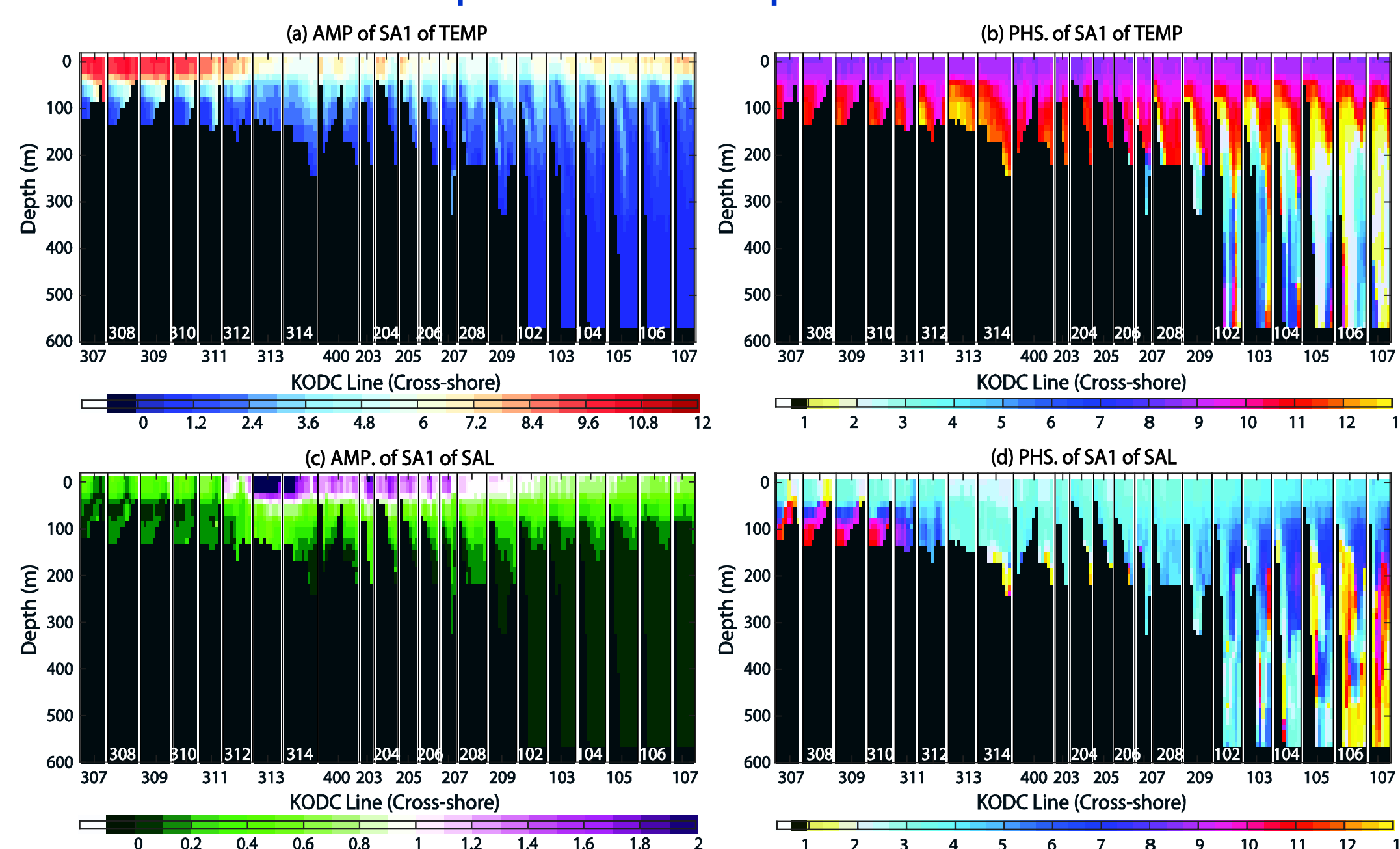


Fig. 3. Seasonal amplitudes and phases of temperature (°C) and salinity profiles for recent 20 years (1995 to 2014)

The annual cycle amplitudes of subsurface temperature for onshore stations (below 50 m from the surface and within 30 km from the coast) at the ES are relatively weak because NKCC move southward all the year (even the width has variability) [e.g., Yun et al, 2004]. Furthermore, there is location of interplay of NKCC and TWC where the phases of annual cycle are abruptly changed and the semi-annual amplitudes are relatively larger (1.7-2.3°C) than around area (0-1.5°C). The offshore stations (30 km from the coast) along the ES indicate concave shape of amplitudes between 150 and 500 m which may related to anticyclonic UWE (The UWE is shown at 500 m [e.g., Shin et al, 1995]).

At the SC, the annual amplitudes of temperature show different pattern between east part (line 206, 207, and 208) and west part (line 204 and 205) because tidal mixing at the west part is stronger than east part which make column uniformly and transfer surface seasonal variability to subsurface [e.g., Kim et al., 2000]. In addition, coastal current along the southwest of Korea has seasonality such as northward warm current during summer and southward cold current during winter [e.g., Pang et al, 1996] which may also generate large seasonal variability at the west part of SC. In addition, the phase is uniform vertically at the coast.

The annual cycle amplitudes of temperature in the surface (upper 30 m) are largest at the YS (> 8°C) since the YS is shallower than 100 m and easy to affected by seasonal variation of solar radiation and wind [e.g., Kang and Jin, 1984; Chu et al, 2004]. The amplitudes at the subsurface (50-70 m) increase toward the coast (e.g., line 307, 308, 309, 310, and 311) due to strong tidal mixing. At the offshore subsurface station (20 km from the coast, under 30 m depth), the annual amplitudes are smaller than same depth of other seas about 2-3 °C but has larger explained variance (>70%).

The annual variability along the ES coast shows that high variability (pink color area) is getting narrowed because the East Korea warm current (EKWC; a branch of TWC) has high salinity variability due to the Chang-jiang river and move northward along the ES coast [e.g., Kang and Jin, 1984]. The low seasonal variability of salinity for onshore subsurface (within 20 km from the coast, between 50 m and 150 m depth) is relatively smaller than offshore about 0.4 due to NKCC like seasonal amplitudes of temperature.

The annual cycle amplitudes of salinity at the SC are largest around Korea since the Chang-jiang river flow to the SC during summer [e.g., Kim et al, 1991].

### 3.3. Diffusivity

From the annual amplitudes and phases, we can obtain the vertical diffusivity (e.g., Kang and Kang, 1987). If the advection can be ignored, the vertical motion can be expressed as (1) and boundary conditions are given as (2).

$$\frac{\partial T}{\partial t} = \kappa \frac{\partial^2 T}{\partial z^2}, \quad (1)$$

$$T = A \cos(2\pi\sigma t) \quad \text{at } z = 0, \quad (2)$$

$$T = 0 \quad \text{at } z = \infty,$$

where  $\kappa$  is diffusivity and  $\sigma = 1/365.2425 \text{ cpd}$ . The solution is shown on (3).

$$T(z, t) = A \exp(-\alpha z) \cos(\omega t - \alpha z), \quad (3)$$

where  $\alpha = (\omega/2\kappa)^{1/2}$ . This solution indicates that the seasonal amplitudes decrease exponentially and phases decrease linearly which is consistent with profiles obtained from CTD (Fig. 4.). Thus, the e-folding decay depth of seasonal amplitudes is  $1/\alpha$  and slope of seasonal phase is  $\alpha$  which can derive diffusivity.

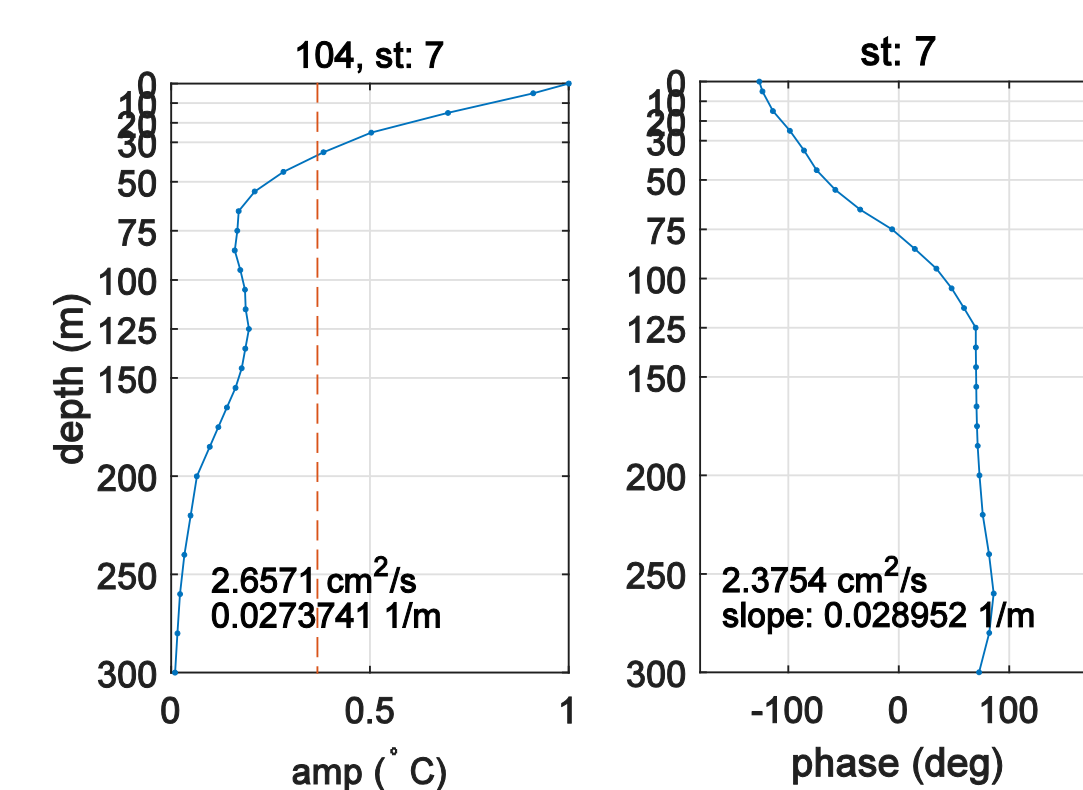


Fig. 4. Example of the seasonal amplitudes and phases profile at line 104 station 7. (The position is indicated at Fig. 5. as red circle)

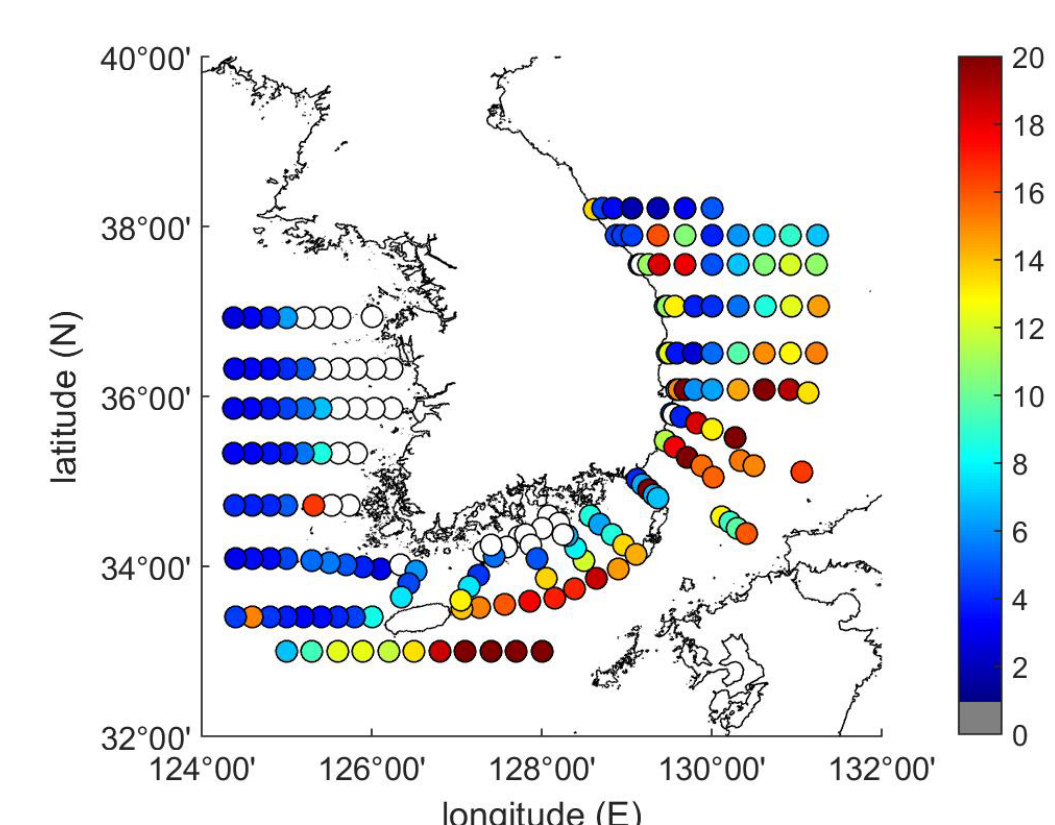


Fig. 5. The diffusivity ( $\text{cm}^2/\text{s}$ ) obtained from e-folding depth of seasonal amplitudes. (When the amplitude can't reach e-folding depth, it is indicated as white color.)

The diffusivity can be obtained from seasonal amplitudes or phases around south Korea (the ES) and shows similar spatial pattern (correlation is 0.24 (0.47)). The vertical diffusivity at the northeast of ES is relatively small ( $< 6 \text{ cm}^2/\text{s}$ ) than the southeast of ES ( $> 10 \text{ cm}^2/\text{s}$ ) because of southward NKCC along the coast. The diffusivity for the offshore stations at the YS is small ( $< 6 \text{ cm}^2/\text{s}$ ) which may be resulted from strong stratification during summer.

## Appendix: Accuracy of seasonal regression

Although the CTD data at a single station have been sampled at every approximately two months, they may not be sampled concurrently and may have missing data. Thus, we evaluate how well the seasonal regression can reconstruct the known seasonal signals with noise and take into account the degrees of mismatch as the errorbar of estimates. A 20-years long time series ( $L = 20$  years) with pure seasonal variance and  $p\%$  of noise is sampled as the CTD data were sampled. To increase the degrees of freedom, the time axis can be generated to have the same probability density function (PDF) of sampling intervals ( $\Delta t$ ) of CTD data by randomly shuffling the time internals.

$$d(t) = \sin(2\pi\sigma t) + \epsilon(t),$$

where  $\epsilon(t) = N(0, p^2)$ ,  $\sigma = 1/365.2425 \text{ cpd}$ . The PDF of time intervals show the 60 days and 10 days of mean and standard deviations, respectively. The time axis can be given by a cumulative sum of sampling intervals:

$$t(k) = \sum_{j=1}^k \Delta t(j), \quad t \leq L.$$

The reconstructed amplitudes along the std of data noise ( $p$ ) are shown in Fig. 5. For example, the accuracy is more than 85% as long as variance explained by regression is larger than 0.5 (Fig. 6).

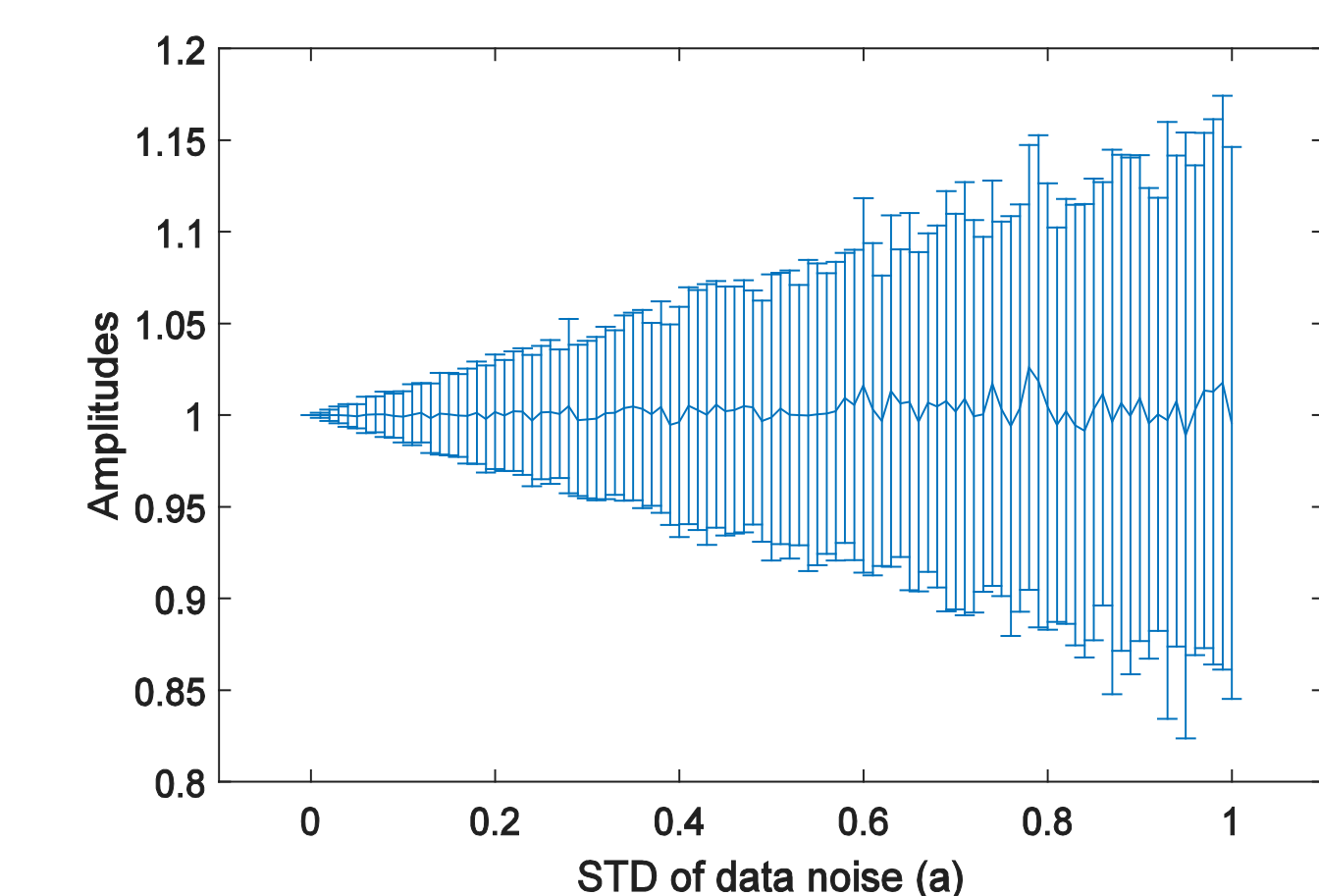


Fig. 6. Reconstructed amplitudes for knowing accuracy of seasonal regression when data is irregularly sampled.

## Acknowledgement

This work is supported by the Human Resources Development of the Korea Institute of Energy Technology Evaluation and Planning (KETEP), Ministry of Trade, Industry and Energy (no. 20114030200040), Republic of Korea.

## References

- [1] C. K. Kim, K. L. Chang, K. Park, and M. S. Suk, The South Sea circulation of Korea: Two-dimensional barotropic model, The J. of the Oceanological Soc. of Korea, 5(4), pp. 257-266, 2000.
- [2] H. J. Lie, S. K. Byum, I. Bang, and C. H. Cho, Physical structure of eddies in the southwestern east sea, The J. of the Oceanological Soc. of Korea, 30(3), pp. 170-183, 1995.
- [3] X. Lü, F. Qiao, C. Xia, G. Wang, & Y. Yuan, Upwelling and surface cold patches in the Yellow Sea in summer: Effects of tidal mixing on the vertical circulation. *Continental Shelf Research*, 30(6), pp. 620-632, 2010.
- [4] J. Y. Na, S. K. Han, and K. D. Cho, A study on sea water and ocean current in the sea adjacent to Korea Peninsula, Journal of the Korean fisheries society, 23(4), pp. 267-279, 1990.
- [5] M. Saraceno, P. T. Strub, and P. M. Kosro, Estimates of sea surface height and near-surface alongshore coastal currents from combinations of altimeters and tide gauges, J. Geophys. Res., 113, 2003, C11013, doi:10.1029/2008JC004756.
- [6] Y. G. Yang, S. H. Kim, and H. K. Rho, A Study on the Temperature fronts observed in the South-West Sea of Korea and the Northern Area of the East China Sea, The Korean Journal of Fisheries and Aquatic Sciences, 31(5), pp. 695-706, 1998.